Clogging Transition of Vibration-Driven Vehicles Passing through Constrictions

G. A. Patterson,[1,*] P. I. Fierens,[1] F. Sangiuliano Jimka,[2] P. G. König,[2]
A. Garcimartín,[3] I. Zuriguel,[3] L. A. Pugnaloni,[4] and D. R. Parisi[1]

[1] *Instituto Tecnológico de Buenos Aires, CONICET, Lavardén 315, 1437 C. A. de Buenos Aires, Argentina*
[2] *Instituto Tecnológico de Buenos Aires, Lavardén 315, 1437 C. A. de Buenos Aires, Argentina*
[3] *Departamento de Física y Matemática Aplicada, Facultad de Ciencias, Universidad de Navarra, Pamplona 31080, Spain*
[4] *Departamento de Ingeniería Mecánica, Facultad Regional La Plata, Universidad Tecnológica Nacional, CONICET, Avenida 60 Esq. 124, 1900 La Plata, Argentina*

We report experimental results on the competitive passage of elongated self-propelled vehicles rushing through a constriction. For the chosen experimental conditions, we observe the emergence of intermittencies similar to those reported previously for active matter passing through narrow doors. Noteworthy, we find that, when the number of individuals crowding in front of the bottleneck increases, there is a transition from an unclogged to a clogged state characterized by a lack of convergence of the mean clog duration as the measuring time increases. It is demonstrated that this transition—which was reported previously only for externally vibrated systems such as colloids or granulars—appears also for self-propelled agents. This suggests that the transition should also occur for the flow through constrictions of living agents (e.g., humans and sheep), an issue that has been elusive so far in experiments due to safety risks.

When a group of discrete rigid bodies is forced to pass through a narrow constriction, undesired flow intermittencies might appear. This phenomenon, which may eventually lead to a complete arrest of the flow, is observed in many different systems across several scales: microbial proliferation [1], colloidal suspensions [2,3], granular materials [4–6], animal flocks [7], and human evacuation [8].

Very recently, a generic clogging phase diagram has been proposed [9] based on a specific property of the intermittencies. When a transient arrest of the flow occurs, the time elapsed until the flow resumes is well described by a power law distribution [10]. However, when the system is flowing, the time it takes until a transient clog forms follows an exponential distribution [10–12]. An order parameter can be defined that weights the relative importance of flowing periods and clogging intervals to assess if a given system is in a clogging state (where the effective mean flow rate is zero in the long term) or in an unclogged state (where the effective flow rate is finite). In practice, the clogging state is observed whenever the exponent of the power law distribution is smaller than -2. Indeed, it has been postulated that the nature of the clogging and unclogging processes can be a universal feature of systems comprising a large number of frictional particles flowing through constrictions. More interestingly, the variables that control clogging in all these disparate systems can apparently be grouped in three different classes [9]: (i) a characteristic size of the constriction, relative to the dimension of the flowing bodies; (ii) a measure of the noise in the motion of the bodies (either intrinsic in self-propelled agents or externally imposed in the case of inert particles); and (iii) a parameter linked to the pressure at the bottleneck. While increasing the width of the constriction and the noise favors the fluidity of the system, increasing the pressure reduces it. This counterintuitive phenomenon has been associated to the *faster-is-slower* effect in pedestrian dynamics, where the evacuation time is minimized for an intermediate value of the driving force [13], and might be behind the fact that an obstacle suitably placed in front of a gate prevents clogging in granular materials [14] and sheep herds [7].

It is a matter of fact that the proposed clogging transition has been observed experimentally only for granular materials in vibrated silos. Experiments with living agents (e.g., humans) are difficult to conduct, and the amount of data that can be gathered is often meager. More importantly, a clogging state implies long-lasting clogs and high pressures at the constriction, which pose a serious risk. In this work, we aim to fill this gap by studying the flow through a bottleneck of macroscopic self-propelled agents. These vehicles have drawn growing attention in recent years because of their complex collective behavior—enriched when the particles are elongated [15,16], polar [17], or when rotation is induced [18]—and for the link that might be established between their behavior and that of active matter [19].

Our self-propelled particles are vibration-driven vehicles (VDVs) commercially available as Hexbug Nano [20] (Fig. 1). Their dimensions are $43 \times 15 \times 18$ mm, and its unidirectional displacement is caused by a vibrating motor and an asymmetric bristle that rectifies the oscillations in the direction of its long axis. The motor is powered by a

1.5 V button cell battery lodged in the body. These VDVs do not have a steering mechanism but can change their bearing when pushed by others or constricted by the geometry of the environment. We drive VDVs through a narrowing by setting an arena with a hopperlike geometry (Fig. 1). It was constructed from wooden walls covered with a PVC sheet and mounted on a metal plate floor. In addition, a glass sheet was placed at a height of 19 mm over the metal base in order to prevent overturning of the VDVs. Among all the system dimensions (given in Fig. 1), the opening size—which is set at $L = 30$ mm, or two agent widths—is the most important for its behavior.

One of the main advantages of VDVs with respect to experiments with living agents (previous studies include humans, sheep, and mice [7,8,21,22]) lies in the amount of data that can be collected. In this regard, we are able to arrange a recirculation of the agents as shown in Fig. 1. Therefore, the experiments can be run for more than 1 hr in steady conditions. In contrast, typical tests performed with sheep or humans last for around 1 min, during which the experimental conditions can hardly stabilize [22,23]. Therefore, we do not need to perform many runs, a scenario in which the statistical analysis may introduce artifacts [24]. In this experiment, the limiting factor was the duration of the batteries. Agents traveling the feedback path that showed signs of a weakened battery were removed. Each experimental realization was ended when 10% of the initial number of VDVs exhausted their batteries. Then, the batteries of all VDVs were replaced before starting a new experimental run.

We have performed experiments with different numbers N of VDVs: $N = 21$ for experiments 1 and 2; $N = 36$ for experiments 3–5, and $N = 51$ for experiments 6–8. A white label with two colored circles was glued to the top surface of the VDVs in order to track their positions and orientations (by means of image analysis performed on every frame of the video recordings) and log the time at which each VDV crossed the exit. Figure 2(a) shows the number of agents egressed as a function of the elapsed time for each independent realization, as well as the mean value computed for each N. Clearly, the larger the number of agents in the arena, the lower the evacuation rate. Although the large temporal scale of Fig. 2(a) does not allow perceiving the short time dynamics, it was observed that the flow of VDVs is intermittent, alternating periods of clogging (or jams) with periods of continuous flow (or bursts), as mentioned above. It can also be observed that experiments with more agents are shorter (less than 5000 s) than those of $N = 21$. This is because for $N = 36$ and $N = 51$ the VDVs remained clogged for longer periods, which quickly dries up the battery. For this reason, when clogs lasted longer than 120 s, we manually released them to prevent long periods of inactivity. These particular events were suitably taken into account when performing the subsequent statistical analysis.

In Fig. 2(b), we show the survival functions [also called the complementary cumulative distribution function (CDF)] of the time lapses Δt between the passage of consecutive VDVs for the three experiments with $N = 36$. The survival function measures the probability $P(T \geq \Delta t)$ that the duration T of a particular clog is greater than or

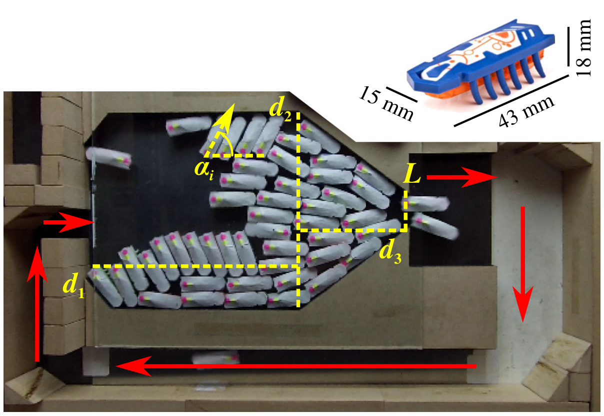

FIG. 1. VDV photograph and snapshot of the system during a typical run. The dimensions are $d_1 = 200$ mm, $d_2 = 180$ mm, $d_3 = 100$ mm, and $L = 30$ mm. Red arrows indicate the feedback path followed by the VDVs. α_i is the angle between agent i and the axis of the enclosure.

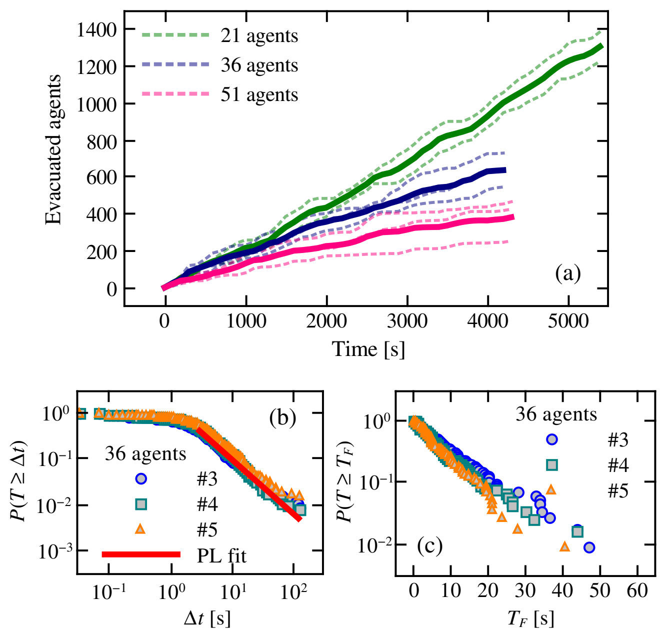

FIG. 2. (a) Number of evacuated agents as a function of the elapsed time for different number of agents in the arena. Dashed lines stand for independent realizations and solid lines for mean values. (b) Complementary CDF of Δt for independent realizations with $N = 36$ agents. Symbols stand for experimental data and the solid line for the fitted power law. (c) Complementary CDF of the burst duration for independent realizations with $N = 36$ agents. Successive bursts are set apart when the time lapse between two consecutive VDVs is longer than 5 s.

equal to a given Δt. Note that we plot the survival function only up to $\Delta t = 120$ s, since at this time clogs were released manually. The results for the three experiments are indistinguishable, stressing the reproducibility of the survival function. We also observe that the tails of the distributions are compatible with a power law (PL) having an exponent γ. Indeed, $P(T \geq \Delta t) \propto \Delta t^{-(\gamma+1)}$ which corresponds to a probability density function $\mathrm{PDF}(\Delta t) \propto \Delta t^{-\gamma}$. We fit the distribution using a well-known technique [25] that, besides γ and the time above which the fit is valid $\Delta t_{\min}$, it quantifies the fit accuracy by means of the p value. The latter is calculated based on the distance between the distributions of the proposed power law and the experimental data. In all cases we find a p value > 0.05, which is the yardstick suggested by the authors of Ref. [25]. $\Delta t_{\min}$ is always between 2 and 5 s and naturally arises as a threshold separating the flowing periods (bursts) from the blocked situations (clogs) during the intermittent flow. In our analysis, if the time interval Δt between successive VDVs is smaller than 5 s, we consider that the flow is continuous and that all the VDVs belong to the same burst. Whenever $\Delta t > 5$ s, we say that the system is transiently clogged. In other words, $\Delta t_{\min} = 5$ s is the threshold time lapse that sets apart successive bursts. As in other systems [9–11], the distribution of burst durations displays an exponential decay [Fig. 2(c)], indicating that the probability of the system getting clogged remains constant over time. Similar results to those shown in Figs. 2(b) and 2(c) were obtained for $N = 21$ and $N = 51$.

In contrast with other studies where the number of agents crowding at the bottleneck decrease with time [7,8,21–23], our feedback mechanism allows us to analyze the effect of the VDVs number, since it is kept within narrow limits. In Fig. 3(a), we show the fitted PL exponent γ for each experimental realization, evidencing that those with the same number of VDVs have similar γ values. Moreover, the larger N, the smaller the exponent. Interestingly, $\gamma \approx 2$ for $N = 51$, which implies that the mean clogging time diverges and the system is said to be in a clogged state [9]. To our knowledge, this is the first case where the transition to a clogged state is experimentally observed in self-propelled agents. In previous works with sheep and humans [8], a tendency towards a clogged state was observed. However, this clogged state was never reached. More precisely, in the case of sheep the lowest PL exponent found was $\gamma = 3.3$, while for pedestrians it was $\gamma = 4.2$, both significantly larger than the critical value of $\gamma = 2$. Although the transition to a clogged state could be expected as it was previously observed in vibrated silos, the fact that it also appears here, where the motion of the particles is not synchronized, widens the scope of this phenomenon.

Apart from the conceptual relevance of the existence of the clogging transition for self-propelled particles, this result has important practical implications. Within the clogged state, any estimation of the flow rate will be ill

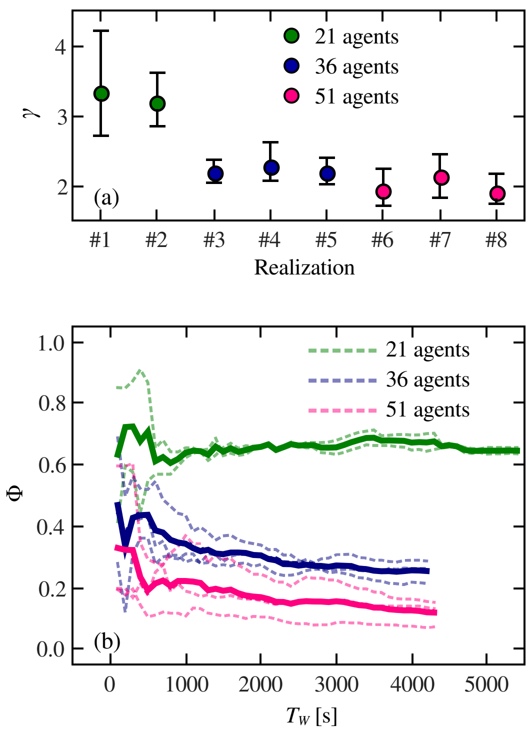

FIG. 3. (a) PL exponent γ for each experimental realization estimated using semiparametric bootstrap methods [25]. Error bars were defined as the 95% confidence intervals. (b) Fraction of time Φ that the system is flowing as a function of the time window T_W in which this magnitude is calculated.

defined, since the result will depend on the width of the time window over which the calculation is done. An example of this is the measurement of the fraction of time that the system is flowing, introduced as the flowing parameter in Ref. [9] as

$$\Phi = \frac{\langle T_F \rangle}{\langle T_F \rangle + \langle T_C \rangle}, \tag{1}$$

where $\langle T_F \rangle$ is the average duration of the bursts and $\langle T_C \rangle$ the average clog duration, both calculated within a temporal window T_W. As a matter of fact, the measured value of Φ strongly depends on T_W if a clogged state is considered [10]. Figure 3(b) displays the value of Φ versus T_W for the eight experiments performed. While for $N = 21$ Φ takes a constant value regardless of T_W, it clearly reduces when increasing T_W for $N = 36$ and for $N = 51$. For $T_W \to \infty$, a distribution PDF $(\Delta t) \propto \Delta t^{-\gamma}$ with $\gamma \leq 2$ leads to $\Phi = 0$. Therefore, from the γ values shown in Fig. 3(a), we know that the asymptotic limit of Φ for $N = 36$ should be a finite number, whereas for $N = 51$ it should be zero.

The density and the spatial correlation of VDVs in the system has been characterized by the radial distribution function $G(r)$, which gives the probability of finding an agent at a given distance from another VDV:

$$G(r) = \left\langle \frac{N(r, r+\Delta r)}{2\pi r \Delta r N_T / S} \right\rangle, \quad (2)$$

where $N(r, r+\Delta r)$ is the number of particles with their geometrical center within $[r, r+\Delta r]$ from a reference particle (we use $\Delta r = 1$ mm), N_T is the number of agents inside the arena, and S is the area of each particle. The $\langle \cdot \rangle$ operator is the time average. To reduce time correlations in the average, we just consider a single snapshot after each VDV exits through the constriction, since the system configuration changes significantly after those events. In Fig. 4(a), $G(r)$ reveals the existence of peaks at $r \approx 15, 30, 45, \ldots$. These peaks correspond, respectively, to arrangements where 2,3,4,…VDVs are aligned side by side. As could be noted, a drawback for the analysis in Fig. 4 arises from the fact that the VDV length (l) and width (w) are commensurable, i.e., $l = 3w$. Indeed, in experiments with the largest N, the peak at $r \approx 45$ mm is higher than the peak at $r \approx 30$ mm, pointing to the development of VDV alignment in a queue (for which $r \approx 45$). Another feature that can be observed in Fig. 4(a) is that $G(r)$ increases with N. This is due to an increase in the size of groups caused by a higher density of agents inside the arena.

Despite the fact that the shape of agents has been proved to be determinant in the properties of bottleneck flow [26–29], measurements of orientation are particularly complex in other systems (e.g., with sheep or humans). In this work, we can readily track the orientations of VDVs. The relative alignment between two VDVs was characterized via the radial orientation function $Q(r)$, which is the probability that two bodies i and j that are at a given distance have the same orientation:

$$Q(r) = \langle \cos[2(\alpha_i - \alpha_j)] | r < r_{ij} < r + \Delta r \rangle_{i>j}, \quad (3)$$

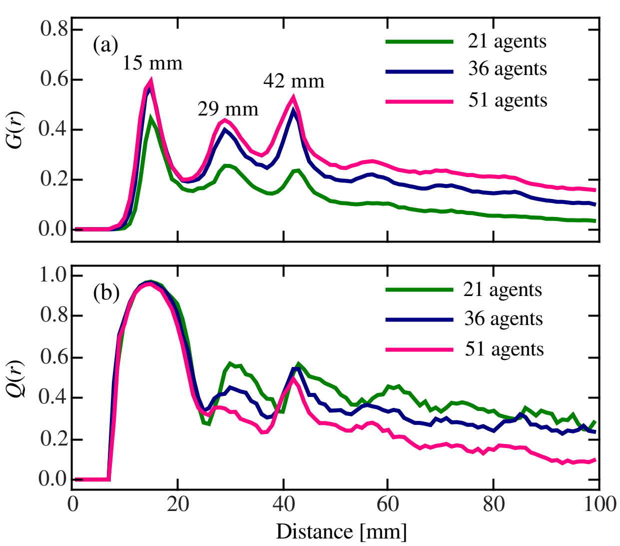

FIG. 4. (a) Radial distribution function and (b) radial orientational function for different N.

where α_i is the absolute orientation of VDV i (see Fig. 1). As for $G(r)$, we use $\Delta r = 1$ mm. Note that when two particles are perpendicular to each other they contribute -1 to $Q(r)$, while when they are parallel the contribution is $+1$. In our experiments we always obtain $Q(r) > 0$ [Fig. 4(b)] due to the marked tendency of VDVs to arrange themselves side by side. Noteworthy, we observe that, for $r \gtrsim 20$ mm, the $Q(r)$ values reduce with N in contrast with the behavior observed in Fig. 4(a) for $G(r)$. Hence, as N increases, the density increases while the prevailing parallel alignment is partially lost. This can be explained if we think that, as the crowd becomes larger, there is an increase of the confinement and the ability of the VDVs to move with respect each other is constrained, reducing the probability of alignment. In this regard, this work underlines the need to better understand the emergence of pressure in dense systems of self-propelled particles. Indeed, it has been recently shown, both theoretically [30] and experimentally [31], that the mechanical pressure in active matter depends on the functional form of the confining potential.

In summary, in this work, we have studied a novel and simple system of self-propelled particles flowing through a bottleneck. There, we can control the number of agents that are involved in the system by means of a feedback path. Our laboratory model is able to reproduce the dynamics of live beings passing through bottlenecks, in particular, those related to the intermittent flow. Indeed, we recover the power law tail distribution for clogging times and the exponential tail for the burst duration. We find that increasing the crowd size is detrimental for the flow as the clog duration becomes longer, up to the point that the transition to the clogged state is reached. This transition, reported previously only for vibrated silos, is therefore revealed to be a general feature of discrete systems passing through constrictions, occurring independently of specific details of the excitation protocol (external or internal, synchronized or unsynchronized). In our experiment, the origin of the clogging transition can be attributed to the augment of the confinement caused by the increment of agents facing the door, in good agreement with the conjecture of the clogging phase diagram [9]. This result can be also seen as a generalization of the faster-is-slower effect where “faster” would mean more pressure, even though this idea needs to be confirmed.

This work was funded by the following projects: ITBACyT-33 (Instituto Tecnológico de Buenos Aires, Argentina); PID2015-003 (Agencia Nacional de Promoción Científica y Tecnológica, Argentina); and FIS2014-57325 (Ministerio de Economía y Competitividad, Spanish Government). G. A. P. acknowledges Fundación Bunge and Born for financial support. A. G. thanks H. Kellay (U. Bordeaux) for general discussions on VDVs. The authors are also grateful to Ariel Robbio, Martín Stortz, and Carlos Stortz for their help with the experiments.

*gpatters@itba.edu.ar

[1] M. Delarue, J. Hartung, C. Schreck, P. Gniewek, L. Hu, S. Herminghaus, and O. Hallatschek, Self-driven jamming in growing microbial populations, Nat. Phys. **12**, 762 (2016).
[2] M. D. Haw, Jamming, Two-Fluid Behavior, and Self-Filtration in Concentrated Particulate Suspensions, Phys. Rev. Lett. **92**, 185506 (2004).
[3] D. Genovese and J. Sprakel, Crystallization and intermittent dynamics in constricted microfluidic flows of dense suspensions, Soft Matter **7**, 3889 (2011).
[4] K. To, P. Y. Lai, and H. K. Pak, Jamming of Granular Flow in a Two-Dimensional Hopper, Phys. Rev. Lett. **86**, 71 (2001).
[5] C. C. Thomas and D. J. Durian, Fraction of Clogging Configurations Sampled by Granular Hopper Flow, Phys. Rev. Lett. **114**, 178001 (2015).
[6] J. Koivisto and D. J. Durian, Effect of interstitial fluid on the fraction of flow microstates that precede clogging in granular hoppers, Phys. Rev. E **95**, 032904 (2017).
[7] A. Garcimartín, J. M. Pastor, L. M. Ferrer, J. J. Ramos, C. Martín-Gómez, and I. Zuriguel, Flow and clogging of a sheep herd passing through a bottleneck, Phys. Rev. E **91**, 022808 (2015).
[8] J. M. Pastor, A. Garcimartín, P. A. Gago, J. P. Peralta, C. Martín-Gómez, L. M. Ferrer, D. Maza, D. R. Parisi, L. A. Pugnaloni, and I. Zuriguel, Experimental proof of faster-is-slower in systems of frictional particles flowing through constrictions, Phys. Rev. E **92**, 062817 (2015).
[9] I. Zuriguel, D. R. Parisi, R. C. Hidalgo, C. Lozano, A. Janda, P. A. Gago, J. P. Peralta, L. M. Ferrer, L. A. Pugnaloni, E. Clément, D. Maza, I. Pagonabarraga, and A. Garcimartín, Clogging transition of many-particle systems flowing through bottlenecks, Sci. Rep. **4**, 7324 (2014).
[10] A. Janda, D. Maza, A. Garcimartín, E. Kolb, J. Lanuza, and E. Clément, Unjamming a granular hopper by vibration, Europhys. Lett. **87**, 24002 (2009).
[11] C. Mankoc, A. Garcimartín, I. Zuriguel, D. Maza, and L. A. Pugnaloni, Role of vibrations in the jamming and unjamming of grains discharging from a silo, Phys. Rev. E **80**, 011309 (2009).
[12] T. Masuda, K. Nishinari, and A. Schadschneider, Critical Bottleneck Size for Jamless Particle Flows in Two Dimensions, Phys. Rev. Lett. **112**, 138701 (2014).
[13] D. Helbing, I. Farkas, and T. Vicsek, Simulating dynamical features of escape panic, Nature (London) **407**, 487 (2000).
[14] I. Zuriguel, A. Janda, A. Garcimartín, C. Lozano, R. Arévalo, and D. Maza, Silo Clogging Reduction by the Presence of an Obstacle, Phys. Rev. Lett. **107**, 278001 (2011).
[15] V. Narayan, S. Ramaswamy, and N. Menon, Long-lived giant number fluctuations in a swarming granular nematic, Science **317**, 105 (2007).
[16] A. Baskaran and M. C. Marchetti, Enhanced Diffusion and Ordering of Self-Propelled Rods, Phys. Rev. Lett. **101**, 268101 (2008).
[17] J. Deseigne, O. Dauchot, and H. Chaté, Collective Motion of Vibrated Polar Disks, Phys. Rev. Lett. **105**, 098001 (2010).
[18] C. Scholz and T. Pöschel, Velocity Distribution of a Homogeneously Driven Two-Dimensional Granular Gas, Phys. Rev. Lett. **118**, 198003 (2017).
[19] C. Bechinger, R. Di Leonardo, H. Löwen, C. Reichhardt, G. Volpe, and G. Volpe, Active particles in complex and crowded environments, Rev. Mod. Phys. **88**, 045006 (2016).
[20] HEXBUG Nano, https://www.hexbug.com/nano.
[21] C. Saloma, G. J. Perez, G. Tapang, M. Lim, and C. Palmes-Saloma, Self-organized queuing and scale-free behavior in real escape panic, Proc. Natl. Acad. Sci. U.S.A. **100**, 11947 (2003).
[22] A. Garcimartín, D. R. Parisi, J. M. Pastor, C. Martín-Gómez, and I. Zuriguel, Flow of pedestrians through narrow doors with different competitiveness, J. Stat. Mech. 2016, 043402 (2016).
[23] W. Liao, A. Tordeux, A. Seyfried, M. Chraibi, K. Drzycimski, X. Zheng, and Y. Zhao, Measuring the steady state of pedestrian flow in bottleneck experiments, Physica (Amsterdam) **461A**, 248 (2016).
[24] A. Nicolas, S. Bouzat, and M. N. Kuperman, Statistical fluctuations in pedestrian evacuation times and the effect of social contagion, Phys. Rev. E **94**, 022313 (2016).
[25] A. Clauset, C. R. Shalizi, and M. E. Newman, Power-law distributions in empirical data, SIAM Rev. **51**, 661 (2009).
[26] J. Tang and R. P. Behringer, Orientation, flow, and clogging in a two-dimensional hopper: Ellipses vs. disks, Europhys. Lett. **114**, 34002 (2016).
[27] T. Börzsönyi, E. Somfai, B. Szabó, S. Wegner, P. Mier, G. Rose, and R. Stannarius, Packing, alignment and flow of shape-anisotropic grains in a 3D silo experiment, New J. Phys. **18**, 093017 (2016).
[28] A. Ashour, S. Wegner, T. Trittel, T. Börzsönyi, and R. Stannarius, Outflow and clogging of shape-anisotropic grains in hoppers with small apertures, Soft Matter **13**, 402 (2017).
[29] R. C. Hidalgo, D. R. Parisi, and I. Zuriguel, Simulating competitive egress of noncircular pedestrians, Phys. Rev. E **95**, 042319 (2017).
[30] N. Nikola, A. P. Solon, Y. Kafri, M. Kardar, J. Tailleur, and R. Voituriez, Active Particles with Soft and Curved Walls: Equation of State, Ratchets, and Instabilities, Phys. Rev. Lett. **117**, 098001 (2016).
[31] G. Junot, G. Briand, R. Ledesma-Alonso, and O. Dauchot, Active versus Passive Hard Disks against a Membrane: Mechanical Pressure and Instability, Phys. Rev. Lett. **119**, 028002 (2017).